Estudio de la estructura electrónica de cristales con lantánidos y actínidos.

J.F. Rivas Silva, IFUAP

Resumen

En esta plática se presentan detalles de los cálculos realizados en modelos de tres casos de materiales en particular: el compuesto ZnO hexagonal dopado con el ion de Europio (ZnO:Eu+2 y +3), los dos metales puros de Plutonio (Pu) y Americio (Am).

En el primero caso se utilizó el programa Crystal para obtener los estados base y excitado del sistema así como el código Wien2k para hacer comparaciones, mientras para los dos segundos se usó principalmente el código Wien2k.

En todos los casos, se resuelven las ecuaciones de DFT ya sea de Schroedinger o de Dirac, y se optimiza la geometría de la celda unitaria, se obtienen las bandas electrónicas y las DOS para obtener conclusiones sobre la estructura electrónica.

Debido al efecto de la alta correlacion en los actínidos, se emplean tanto la aproximación GGA+U que agrega una corrección de tipo Hubbard al hamiltoniano de DFT, como funcionales híbridos convenientes (eece) para considerar el mismo efecto. Se consideran los criterios de estabilidad elásticos para lograr comparaciones con los datos experimentales fundamentales.

1. Kondo-Like Resonance in ZnO:Eu
A. BLANCA-ROMERO, M. BERRONDO, J. F. RIVAS-SILVA , International Journal of Quantum Chemistry, Vol 111, 3831–3840 (2011)

Supercell structure (de una hexagonal spatial group: P-1)

Lattice parameters

a (Å) b (Å)c (Å)

6.49854 6.49854 5.20544

Angles α β γ

90 ◦90 ◦120 ◦

No. of atoms

Zn O Eu
7 8 1

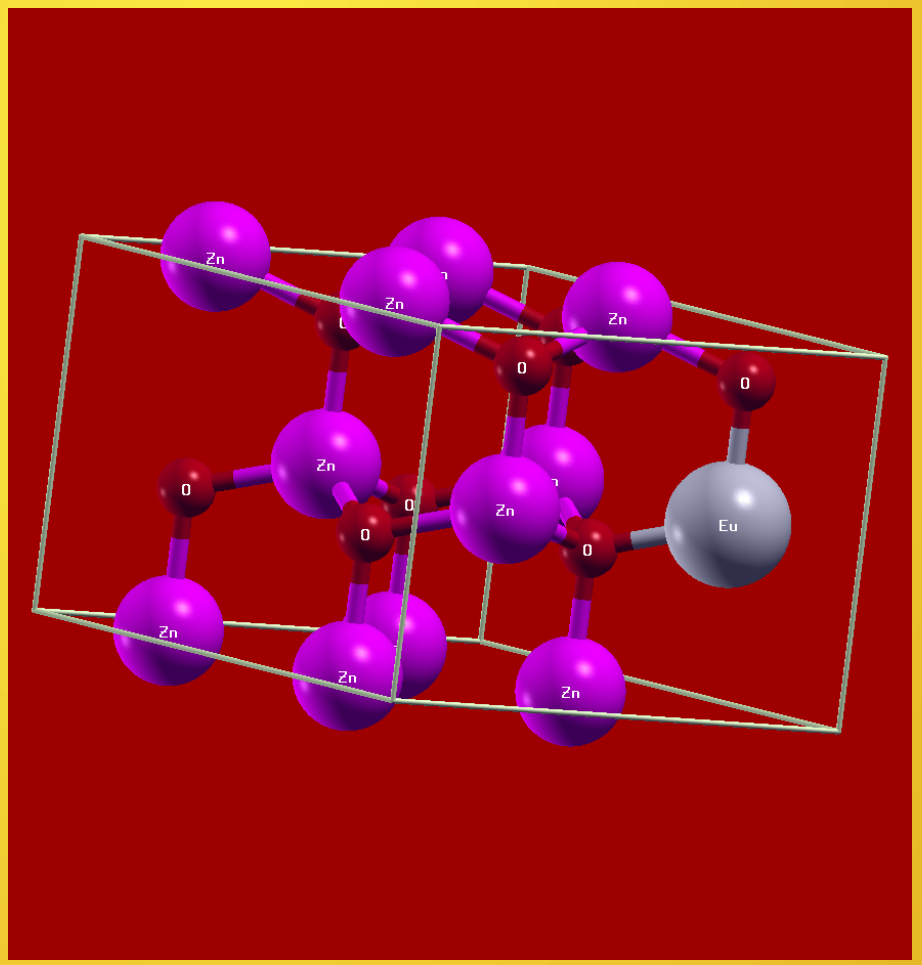

WIEN2K CALCULATIONS

MFT (Division of the space between spheres and an interstitial zone, radius (Bohrs))
LAPW:

$$\phi_{lm} = \sum_{lm} \left[A_{lm,\mathbf{kn}} u_l(\mathbf{r}, E_l) + B_{lm,\mathbf{kn}} \dot{u}_l(\mathbf{r}, E_l) \right] Y_{lm}(\mathbf{r}),$$

espacio entre esferas de *muffin-tin*, conocido como región intersticial [90]:

$$\phi_{kn} = \frac{1}{\sqrt{\omega}} e^{i\mathbf{k}_n \cdot \mathbf{r}}. \qquad (3.2)$$

(Zn, 1.77), (O, 1.57) and (Eu, 1.77).
Number of k points 1000.65 NM

Functional
GGA (Generalized gradient approximation of Perdew- Burke-Ernzerhof 96)

CRYSTAL06

PS de cep-121 gaussian adaptado.
Se usó un DFT híbrido para simular el efecto de la U de Hubbard de Wien2k,

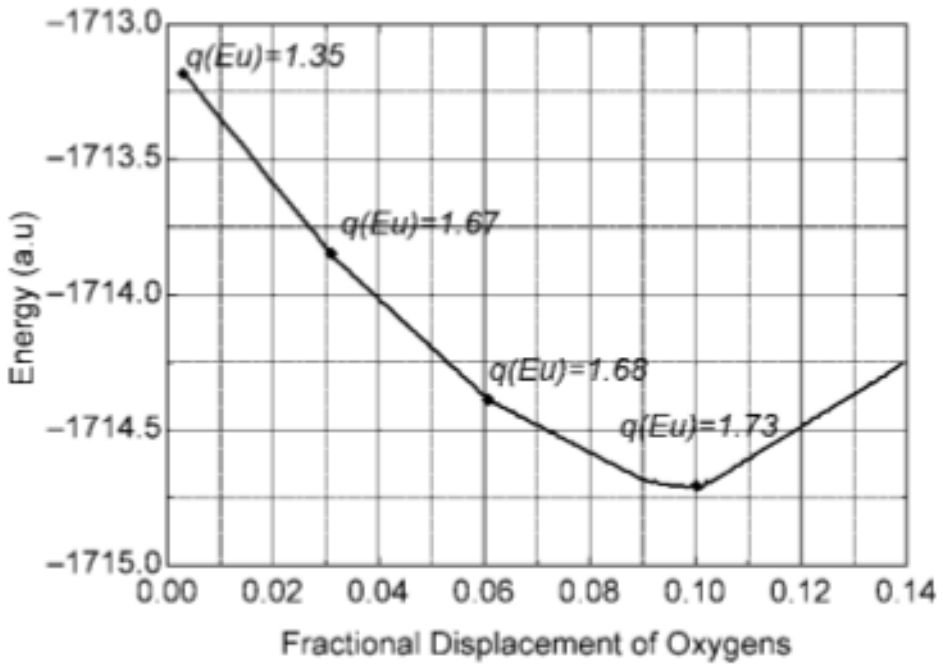

FIGURE 11. Energy versus displacement ZnO:Eu^{2+}.

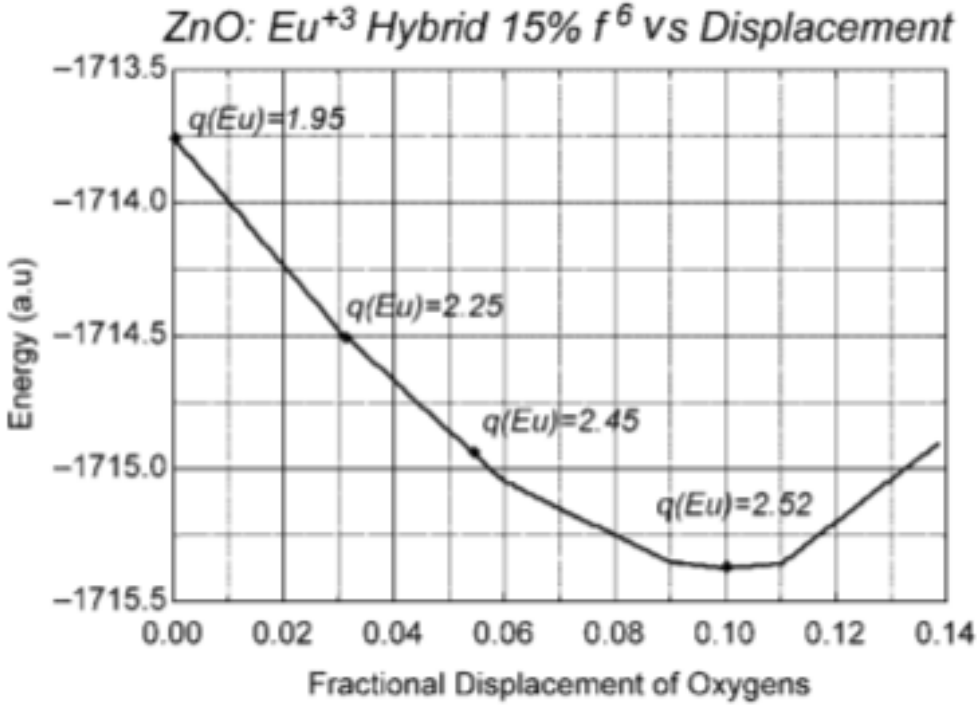

FIGURE 12. Energy versus displacement ZnO:Eu^{3+}.

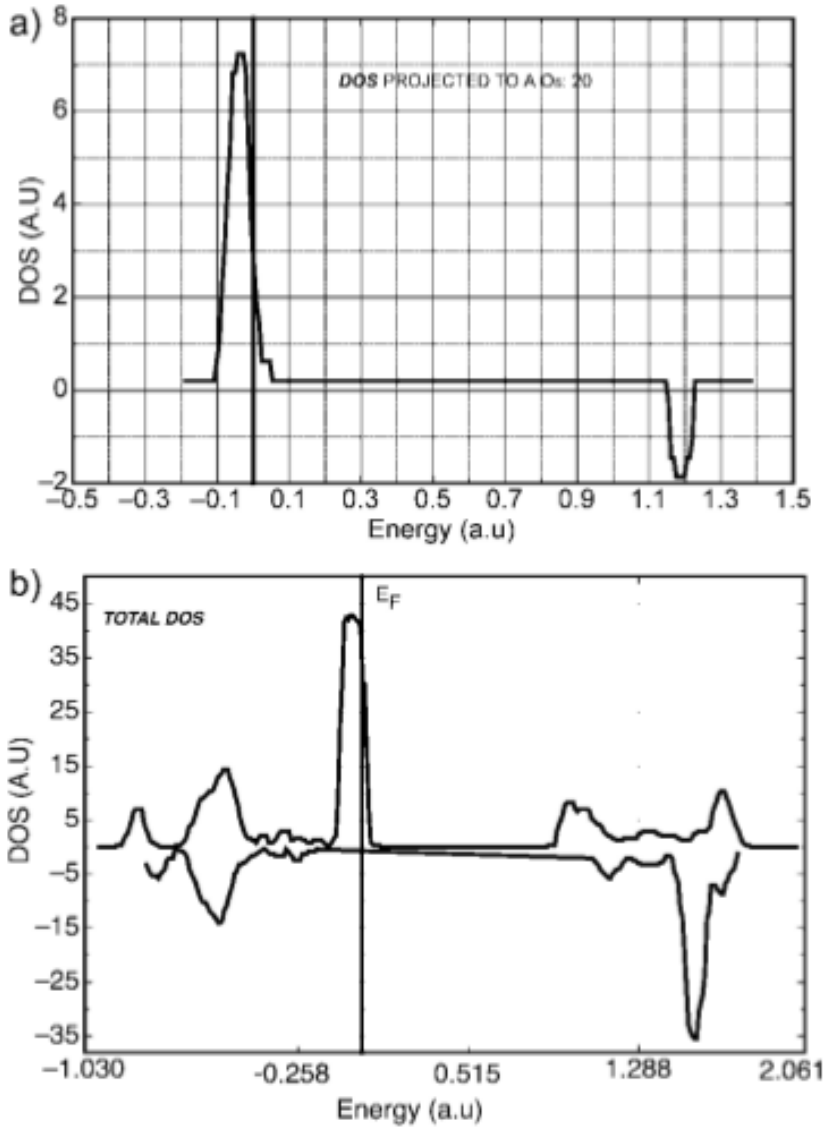

FIGURE 10. (a) *f* states DOS of Eu^{2+} in $ZnO:Eu^{2+}$. (b) Total DOS of $ZnO:Eu^{2+}$. The resonance in (b) appears on top of the Fermi energy and (a) shows that it is formed mostly by *f* levels from the Eu; α states are plotted above and β states below the level line.

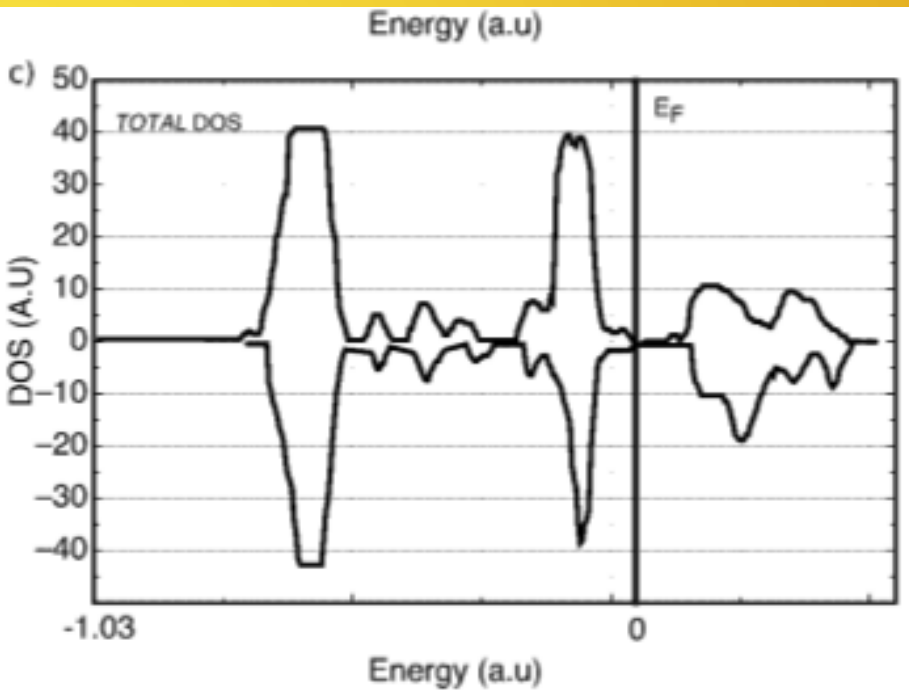

FIGURE 13. (a) The total DOS of the Zn^{2+} in $ZnO:Eu^{3+}$. (b) The total DOS of the Oxygen in $ZnO:Eu^{3+}$. (c) The total DOS of the crystal $ZnO:Eu^{+3}$. These DOS show that the O and Zn states do not have contributions in the Fermi energy zone; α states are plotted above and β states below the level line.

The calculations made with CRYSTAL06 allow us to obtain the first optical absorption of the system theoretically. This corresponds to the observed ${}^{7}_{0}F \rightarrow {}^{5}_{2}D$ transition. The difference between the f^6 and f^4 states energy curves has been obtained assuming a vertical transition and using the 15% mixture of exchange and DFT potentials. A calculated value of ~2.5 eV results, compared with an experimental one of ~2.6–3.1 eV.

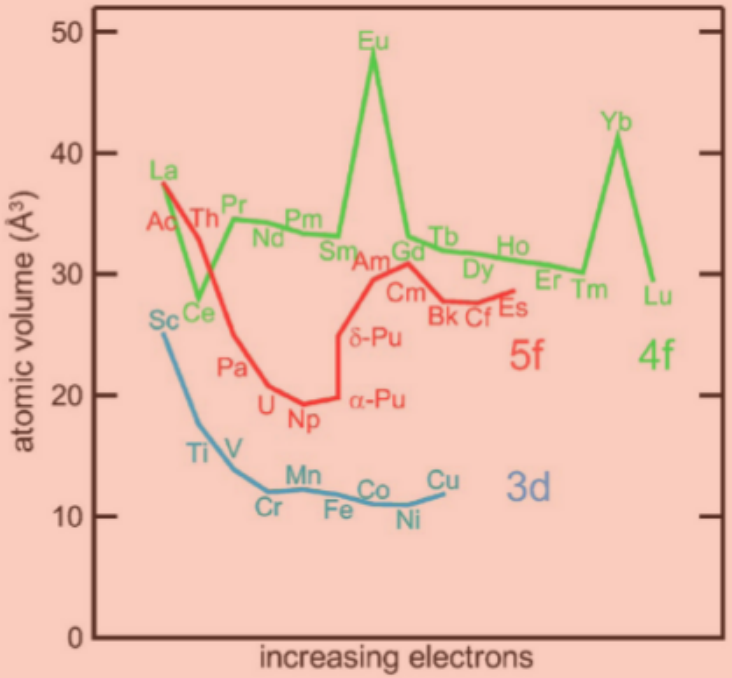

Figura 1.1.1: Figura tomada de **[30]-Fig. 1.** Comparación de los volúmenes por atómo entre lantánidos (verde), actínidos (rojo) y metales de transición (cyan), como función de un incremento de los estados de valencia (hacia la derecha).

2. Ground state stability of dPu by way of introducing exact exchange within a DFT potential for correlated electrons
J.J. Ríos-Ramírez ⇑ , J.F. Rivas-Silva, A. Flores-Riveros

Computational Materials Science 126 (2017) 12–21

Pu fcc, i.e. fase delta
Wien2k.

Para tal fin el espacio cristalino real es dividido en regiones esféricas no traslapadas de radio Rmt alrededor de cada átomo, llamadas esferas de muffin-tin.
The muffin-tin radius is equal to Rmt 2.7 a.u.
Bravais lattice 1000 k points

Métodos: DFT híbrido eece (pbe+ corrección al exchange de los electrones f) +SO vs. GGA+U.

Experimental: estado base no-magnético!
Todos los DFT standard, obtienen un edo. magnético. También GGA+U.
Variando el parámtro del eece, alpha se tiene un NM GS a 0.65
Es casual?

CRITERIO FUNDAMENTAL: Propiedades elásticas:

$c11 > |c\ 12|,\ \ c11 + 2c12 > 0,\ \ c44 > 0$

polarización de espín y tomando en cuenta el acoplamiento espín-órbita del Hamiltoniano relativista [93]:

$$\left[\frac{\mathbf{p}^2}{2m} + V(\mathbf{r}) - \frac{\mathbf{p}^4}{8m^3c^2} - \frac{\hbar^2}{4m^2c^2}\frac{dV}{dr}\frac{\partial}{\partial \mathbf{r}} + \frac{1}{2m^2c^2}\frac{1}{r}\frac{dV}{dr}(\mathbf{L}\cdot\mathbf{S})\right]\Psi = \varepsilon\Psi, \tag{3.11}$$

$$E_{xc}^{eece}[n(\mathbf{r})] = E_{xc}^{PBE}[n(\mathbf{r})] + \alpha\left(E_x^{HF}[\Psi_{corr}] - E_x^{PBE}[n_{corr}]\right),$$

$$E = E^{PBE} - E^{dc} + \frac{1}{2}U\sum_{m,m',\sigma} n_{m\sigma}n_{m'-\sigma} + \frac{1}{2}(U-J)\sum_{m\neq m',m',\sigma} n_{m\sigma}n_{m'\sigma}, \tag{3.13}$$

con un término de doble conteo que depende del número total de electrones como: ($N = \sum_{m,\sigma} n_{m\sigma}$) escrito como [81]:

$$E_{dc} = \frac{1}{2}UN(N-1) - \frac{1}{4}JN(N-2), \tag{3.14}$$

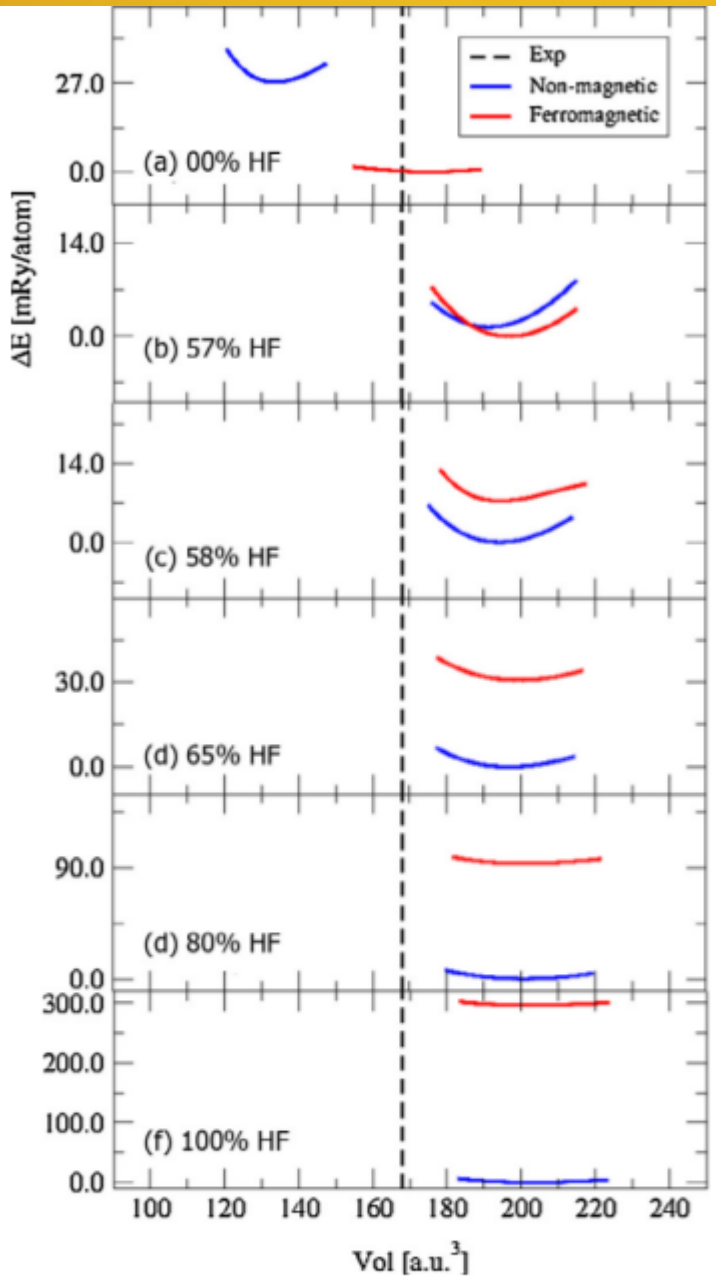

Fig. 1. Total energy values for isotropic deformation computed under the LAPW+SO +α scheme as a function of the unit cell volume fitted by the equation of state with values: $\alpha = 0.00, 0.57, 0.58, 0.65, 0.80$ & 1.00. In agreement with previous studies at $\alpha = 0.00$ the volume of the Non-Magnetic phase is severely underestimated while the ferromagnetic state is in good agreement with the experimental value [25]. The transition is expected to occur at 57% where a crossing point is found at approximately $a = 4.82$ Å.

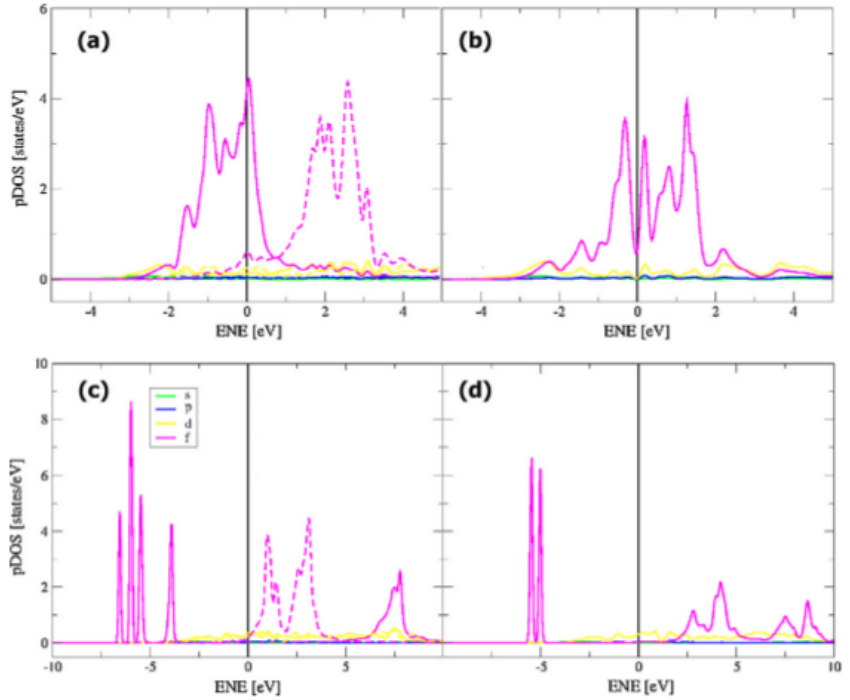

Fig. 2. Projected density of states computed under the LAPW+SO+α scheme for (a) Ferromagnetic (FM) and (b) Non-Magnetic (NM) configurations, with $\alpha = 0.00$ and and (d) NM, with $\alpha = 0.65$. Solid and broken lines indicate spin-up spin-down polarization, respectively.

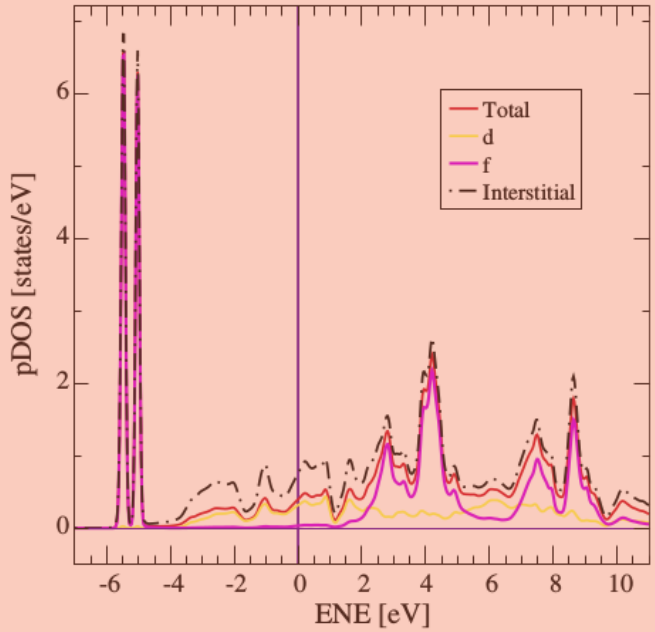

Fig. 4. PDOS computed under the LAPW+SO+α scheme for a Non-Magnetic (NM) configuration at $\alpha = 0.65$. Solid and dashed-dotted lines indicate spin-up polarization inside the muffin-tin sphere and at interstitial states, respectively.

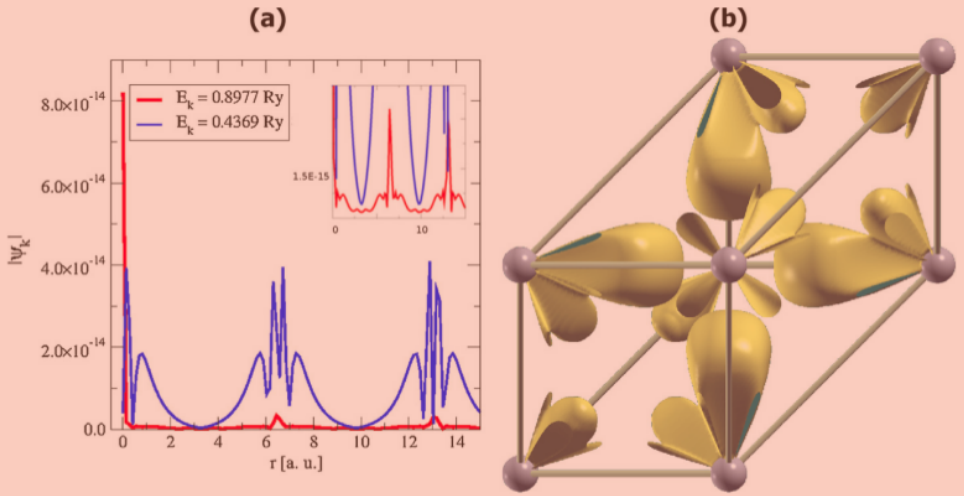

Fig. 5. (a) Absolute value of the large component of Ψ_k calculated under the LAPW+SO+α scheme for Non-Magnetic (NM) configuration at $\alpha = 0.65$. The energy values correspond to states inside the valence band (blue) and near the Fermi level (red) at Γ point ($E_{Fermi} = 0.85$ Ry). (b) Valence spin density distribution for the Non-Magnetic (NM) configuration with $\alpha = 0.65$ parallel to the *XY* plane. (For interpretation of the references to color in this figure legend, the reader is referred to the web version of this article.)

- Estudio de propiedades elásticas:

$$\begin{pmatrix} \mathbf{x}' \\ \mathbf{y}' \\ \mathbf{z}' \end{pmatrix} = (\mathbf{D}(e) + I) \begin{pmatrix} \mathbf{x} \\ \mathbf{y} \\ \mathbf{z} \end{pmatrix},$$

Table 2
Bulk Modulus, Shear Modulus and Cubic Elastic Constants of δPu at each spin configuration computed under the LAPW+SO+α scheme by a finite deformation method. The mechanically stable structures are located at α values around the magnetic ground state transition. The Non-Magnetic configuration shows a tetragonal instability [$c_{11} < |c_{12}|$] at $\alpha = 0.00$ & 1.00, and another instability [$c_{44} < 0$] at $\alpha = 0.57$, 0.58 & 0.80. For the Ferromagnetic configuration such instabilities occur at $\alpha = 0.57$, 0.80 & 1.00 and $\alpha = 0.00$ & 0.57, respectively. These quantities are compared with previous calculations [11,20,24] and experimental measurements at room temperature and at the δPu phase transition temperature [26].

α	Mag.	V [a.u.^{3}]	B	c'	C_{11} [GPa]	C_{12}	C_{44}
0.00	NM	134.01	92.70	−35.08	45.92	116.08	149.07
	FM	172.06	19.81	3.09	23.94	17.74	−14.50
0.57	NM	194.07	80.52	1.95	83.12	79.21	−150.89
	FM	195.62	84.60	−1.08	83.15	85.32	−25.06
0.58	NM	194.46	80.74	2.93	84.65	78.77	−21.71
	FM	197.86	66.17	0.74	67.16	65.67	170.86
0.65	NM	196.73	79.48	1.79	81.86	78.27	134.23
	FM	197.02	78.71	3.22	83.01	76.55	32.50
0.80	NM	199.48	84.55	1.29	86.27	83.68	−292.97
	FM	201.63	73.79	−1.60	71.64	74.85	44.57
1.00	NM	203.17	78.68	−1.19	77.08	79.47	86.45
	FM	203.56	75.83	−0.40	75.28	76.09	92.31
[11]	D	168.20	41.00	18.00			48.00
	FM	172.93	26.00	17.00			27.00
	NM	120.24	165.00	−69.00			15.00

3.Comparing two high correlation models to test the mechanical stability of Americium-II, J.J. Ríos-Ramírez, J.F. Rivas-Silvaa , A. Flores-Riveros, Hérnandez-Cocoletzi, enviado al JP: CM (2018).

“In this work two high correlation methodologies to DFT, a DF T + U implementation and a hybrid DFT functional, with a varying amount of Hartree-Fock exchange α (here utilized in a parametric fashion), are tested”...

The Am-II phase was modelled via the conventional face-centered cubic structure (F m − 3m)-

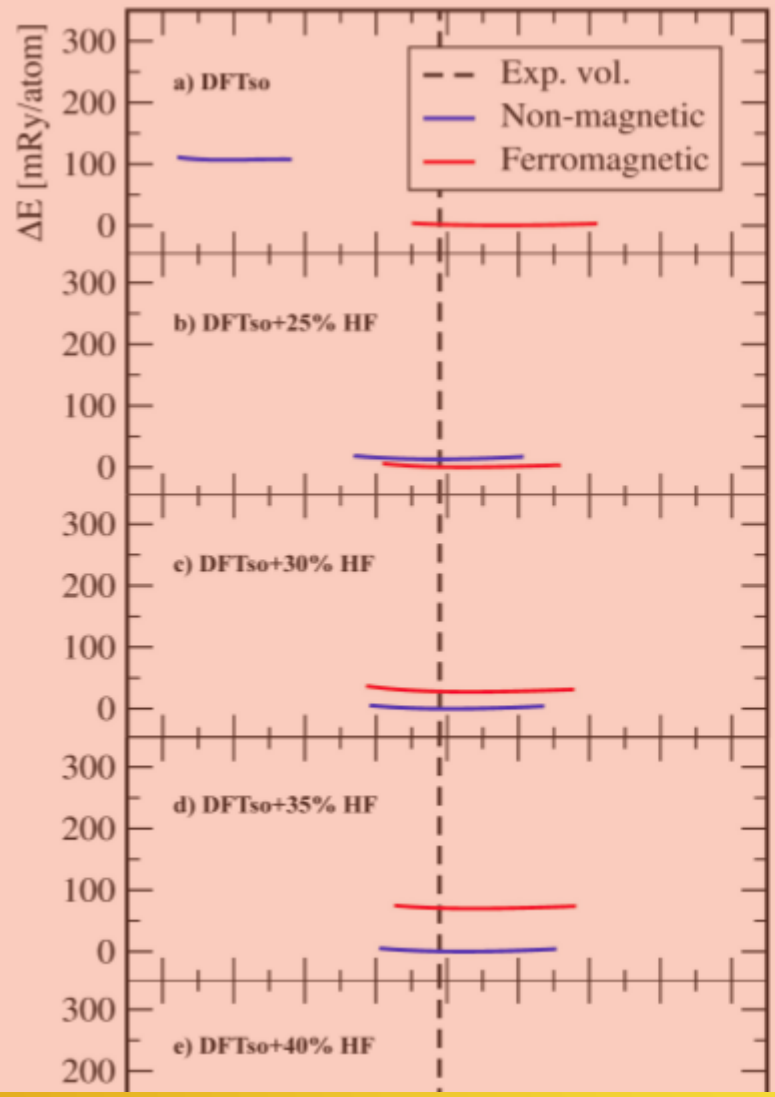
ΔE [mRy/atom]
300
200
100
0
a) DFTso
Exp. vol.
Non-magnetic
Ferromagnetic
b) DFTso+25% HF
c) DFTso+30% HF
d) DFTso+35% HF
e) DFTso+40% HF

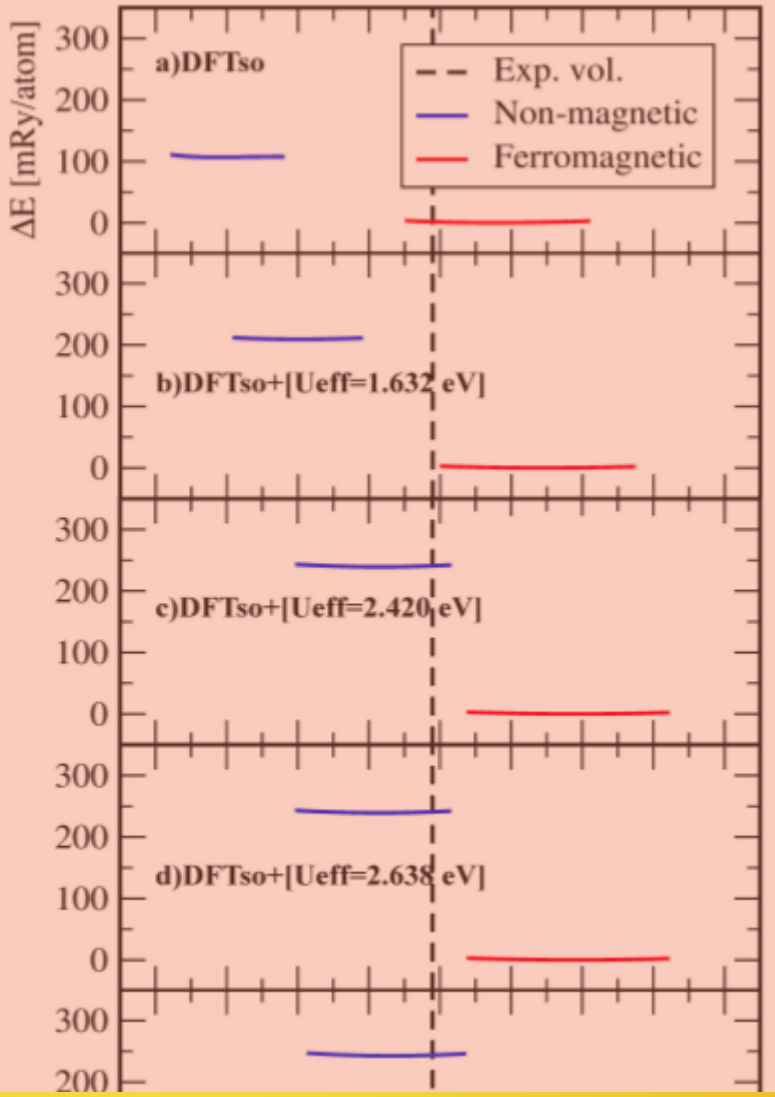
ΔE [mRy/atom]
300
200
100
0
a)DFTso
Exp. vol.
Non-magnetic
Ferromagnetic
b)DFTso+[Ueff=1.632 eV]
c)DFTso+[Ueff=2.420 eV]
d)DFTso+[Ueff=2.638 eV]

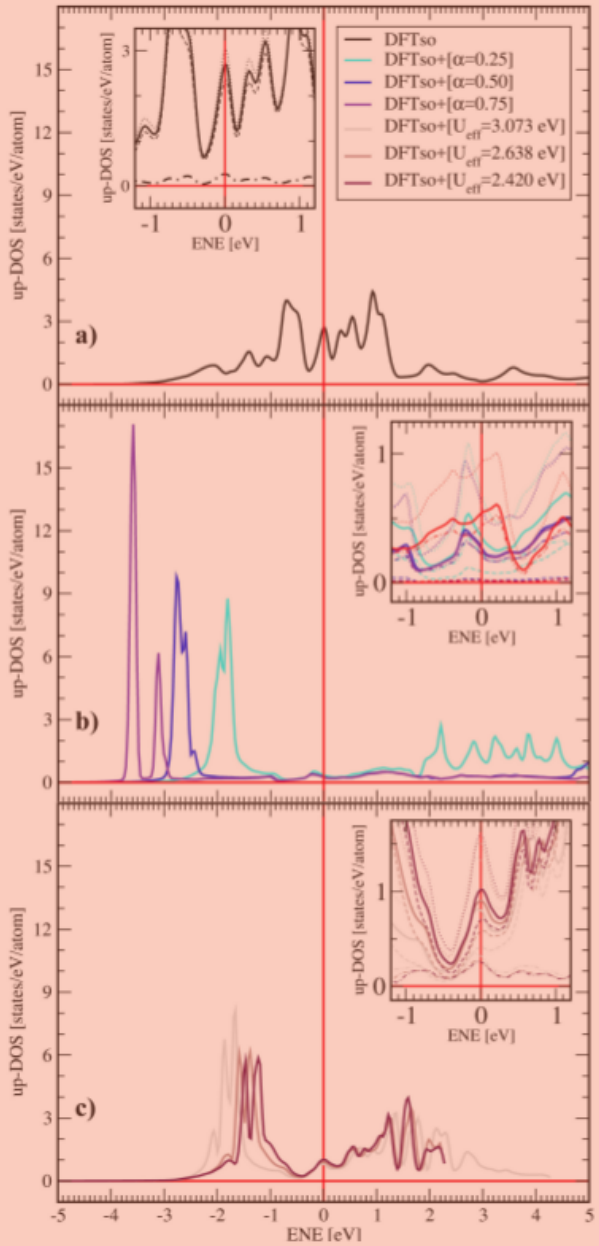

Figure 3.3: Partial density of states of Am-II in the Non-magnetic configuration, under DFTSO (a), HYB-DFT (b) and DFT+U (c). The dashed-dotted lines indicate *d* projec-

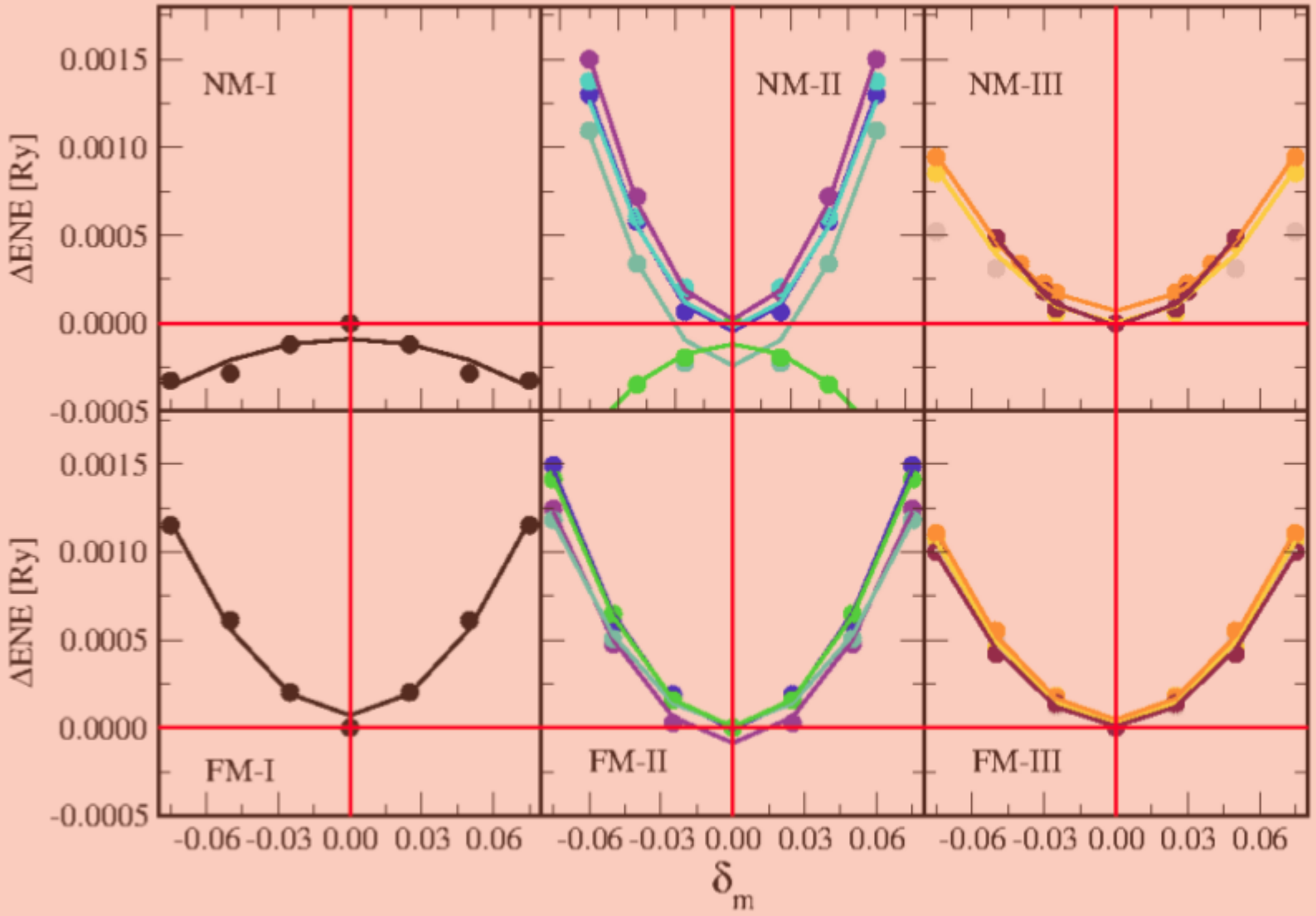

Figure 3.6: Volume conserving monoclinic distortion curves, for the three methodologyical schemes (DFTSO-I, HYB-DFT-II and DFT+U-III) for both configurations. For each α parameter: 0.25 (indigo), 0.40 (blue), 0.55 (cyan), 0.75 (turquoise) and 1.00 (dark-green). The U_{eff} in eV: 3.51 (maroon), 2.64 (orange), 2.42 (yellow) and 1.63 (grey) (For interpretation of the references to color in this figure legend, the reader is referred to the web version of this article).

	FM	30.52	22.22	26.86
HYB-DFT [α]	**Mag.**	c_{11}	c_{12} [GPa]	c_{44}
0.25	NM	76.44	35.16	39.63
	FM	68.28	28.48	33.31
0.40	NM	64.19	36.74	34.16
	FM	47.28	16.10	36.63
0.50	NM	60.54	31.70	31.56
0.55	NM	64.76	30.73	33.27
0.75	NM	60.04	28.46	31.71
	FM	78.78	78.41	31.30
1.00	NM	79.46	106.43	-17.69
	FM	57.29	70.38	37.20
DFT+U [U -V]	**Mag.**	c_{11}	c_{12}	c_{44}

Although, the mechanical stability conditions for the FM configuration are fulfilled using the GGA+U, the set of c ij values is smaller in magnitude, so the best method working is the eece.

Gracias a Ustedes, a los organizadores, a la BUAP y a la Red De Físico-Química Teórica.